Studies in Knowledge and Innovation
Vol. 2 No. 4A (2026)

Reconstructing Chords from Apollo Rover Readouts under Two Display-Cell Assumptions

Simon Hayes[1] · Liam Hall[2] · Evan Anderson[3]

[1] Spain · [2] Portugal · [3] Austria

Published: April 30, 2026 | Article 846

Abstract

Drawing a segment between archived rover coordinates can suggest more geometric precision than the published readouts contain. We audited nine Apollo 15–17 polar-navigation tables and retained 237 comparable adjacent pairs from 281 source rows. Two fixed reconstruction assumptions assign nearest-rounding or lower-bin cells to the documented one-degree and 100 m display increments. Analytically constructed chord envelopes averaged 175.554 m wide under nearest rounding and 179.344 m under lower-bin truncation, with equal mission and traverse weights. Among 197 positive printed chords, 33 had a zero distance infimum under both assumptions. Deleting one mission gave nearest-rounding mean widths of 172.242–177.662 m. These conditional envelopes describe published numerical representations; they are not bounds on actual localization error, probabilities of movement or estimates of driven distance.

Reconstructing Chords from Apollo Rover Readouts under Two Display-Cell Assumptions

Abstract

Drawing a segment between archived rover coordinates can suggest more geometric precision than the published readouts contain. We audited nine Apollo 15-17 polar-navigation tables and retained 237 comparable adjacent pairs from 281 source rows. Two fixed reconstruction assumptions assign nearest-rounding or lower-bin cells to the documented one-degree and 100 m display increments. Analytically constructed chord envelopes averaged 175.554 m wide under nearest rounding and 179.344 m under lower-bin truncation, with equal mission and traverse weights. Among 197 positive printed chords, 33 had a zero distance infimum under both assumptions. Deleting one mission gave nearest-rounding mean widths of 172.242-177.662 m. These conditional envelopes describe published numerical representations; they are not bounds on actual localization error, probabilities of movement or estimates of driven distance.

A printed coordinate is a numerical representation

Historical rover navigation reports provide unusually direct evidence of the numbers available during a lunar traverse. NASA's 1973 review preserves bearing and range readouts, event annotations and navigation-system documentation for all nine Apollo 15-17 traverses (Smith and Mastin, 1973). Those numbers can be converted into points and connected into a map. The resulting line, however, is a construction from discrete readouts rather than a continuous record of wheel motion.

The distinction matters when mission documents become numerical inputs to later reasoning tasks. Lunar-R1 names navigation among the five core scenarios in its Lunar-QA development account (Xiao et al., 2026). That domain provides a limited motivation for preserving what an archived navigation input actually says. Our study does not test that model, estimate its localization ability or use its hardware benchmarks. It examines the information supplied before any model would receive a question.

The measurand must be specified first: here it is the separation between two represented local positions. Metrology distinguishes a quantity intended for measurement from its reported value (JCGM, 2012). We express separation in metres and bearings in angular units consistent with the SI system (BIPM, 2019). We do not call the separation an odometer distance. A numerical scale can support valid arithmetic while still representing a different property from the one a user intended (Stevens, 1946).

Two propositions organize the study. P1 concerns the finite distance information that follows from published polar values when a display-cell assumption is specified. P2 concerns how changing that assumption affects the same finite set of source pairs. Neither proposition predicts a causal vehicle response. The empirical results are the actual envelope widths, their variation across traverses and their composition sensitivity; the geometric identities used to calculate them are not discoveries about the rover.

Rebuilding the source without filling its gaps

The acquired source is NASA Technical Note D-7469, November 1973, by Earnest C. Smith and William C. Mastin. Its official NTRS record labels distribution Public and copyright Work of the US Government, Public Use Permitted. The downloaded PDF has 60 pages and 3,418,450 bytes. The original file, official metadata, source-page renderings and checksum remain in the local provenance record. The source is an archival tabulation of navigation readouts, not a newly collected survey or raw wheel-pulse telemetry.

We audited Tables 5-7, 10-12 and 15-17 against all fifteen original readout pages. They contain 281 rows, including events with blank coordinates. Of these rows, 258 provide both numerical polar fields. The audit preserves the original strings, order, page and table references. One numerical parser rejection was corrected from the printed value 1.9 with trailing punctuation. Two time strings were recovered visually, while their original extraction remained attached. Time is not an outcome in this analysis.

Two printed range headers require explicit interpretation. Table 7 labels range as degrees despite metre-sized Apollo 15 values. Adjacent Apollo 15 tables specify metres, the display documentation uses 100 m increments, and its traverse figure shows a kilometre scale and an extent of about two kilometres. Those sources support reconstructing the Table 7 values as metres. Table 10 has the same header defect, but its continuation explicitly says kilometres. Apollo 16-17 values were converted from kilometres to metres. These are documented unit interpretations, not silently corrected source labels.

Bearing denotes direction to the initialized reference relative to north; it is not vehicle heading. For east and north coordinates, respectively, the reconstruction is $x = -r \sin(b)$ and $y = -r \cos(b)$, with b converted to radians. The PDS Geosciences Node describes this conversion in its map-generation guide (PDS Geosciences Node, n.d.). That guide reconstructs traverses from the same historical readouts. Its map therefore cannot independently establish the accuracy of the positions from which it was built.

The reference is not uniformly the lunar module. Apollo 15 traverse III was initialized at ALSEP, and the Apollo 17 traverses at SEP. Preinitialization Apollo 17 values remain in the audit with an unverified frame. We compare only immediately adjacent rows with complete polar values and a documented common frame. Missing-coordinate rows break adjacency. We also omit the edge spanning the Apollo 15 traverse II heading update, retaining separate calibration epochs without treating them as separate traverses.

This leaves 237 supported pairs: the other rows represent nine first-row states, 26 missing-endpoint pairs, one update boundary and eight unverified-origin or reset states. Arrival/departure duplicates and alignment-check duplicates remain. The Apollo 16 loss-of-navigation note also remains, without interpreting the last repeated display as verified localization. Different initialization clocks in two Apollo 17 tables are preserved; no elapsed-time correction is needed to compute ordered geometry.

A common translation of both endpoints would leave a chord unchanged. A reset between endpoints creates a different problem: the two numerical vectors no longer necessarily refer to the same point on the surface. Treating their origins as identical could turn a bookkeeping change into apparent displacement. Excluding such an edge preserves this distinction without estimating an unavailable origin offset. It also leaves a visible break rather than a visually complete reconstructed route.

Two explicit assumptions about the display cells

Wheel odometry errors can arise from physical and systematic mechanisms that require their own measurements and correction models (Borenstein and Feng, 1996). The NASA report also describes a computational chain using incremental motion, coordinate accumulation and polar conversion. Its reference to the CORDIC technique concerns that conversion, whose general computing method predates these missions (Volder, 1959). Our calculation starts from the published outputs and does not reconstruct this instrument chain or calibrate its physical errors.

Table 1 of the NASA report distinguishes display resolution from accuracy and specifies one-degree bearing and 0.1 km range increments. The record does not establish a publication-wide rounding policy. Quantization theory provides both deterministic mappings and statistical descriptions (Gray and Neuhoff, 1998). Classic work on quantized-signal spectra (Bennett, 1948) and broader treatments of roundoff and

quantization noise (Widrow and Kollár, 2008) concern assumptions that are not automatically supplied by an integer printed angle. We do not assign uniform random errors or a noise spectrum to these records.

We instead fix two alternative reconstruction scenarios. Under N, the nearest-rounding scenario, each printed radius r represents the closed interval from max(0, r-50) to r+50 m, and each bearing b represents b±0.5 degrees. Under T, a lower-bin or truncation scenario, the intervals are r to r+100 m and b to b+1 degree. T uses closures when reporting infima and suprema of the corresponding half-open cells. Both scenarios apply to all supported readouts, including zero ranges and initialization readouts. They describe the published representation, not an assertion that reset registers physically wandered within those cells.

Angles are circular: zero and 360 degrees identify the same direction. Directional analysis requires respecting that periodic structure (Mardia and Jupp, 1999). We canonicalize printed bearings modulo 360 and retain circular sectors when a cell crosses the boundary. No average of raw degree labels replaces a circular calculation. The paired geometric problem is distance between two annular sectors, a finite planar geometry problem (de Berg et al., 2008).

For each endpoint, every radius and bearing in its specified cell is admitted. The pair calculation uses the Cartesian product of those cells. This is an assumption about admissible representations, without a claim that the two instrument errors are stochastically independent. It omits joint restrictions that the complete navigation system or continuous motion might impose. Introducing those restrictions would require information beyond the archived table.

The resulting set answers a deliberately limited compatibility question. It includes all combinations permitted by the separately specified cells, even if a detailed model of the instrument would connect consecutive values more tightly. A smaller physically informed set might follow from known counter states or a complete motion record, but neither is supplied for these printed pairs. Conversely, unspecified drift or transcription mistakes could place actual positions outside the assumed cells. Thus a mathematically exact envelope can be both reproducible and incomplete as a statement about physical location.

Solving the chord envelope and specifying the summary

Let the shorter separation of the two printed bearings be s. Both scenarios allow relative angular separations between max(0, s-1 degree) and min(180 degrees, s+1 degree). Shifting both T angle cells by half a degree is a common rotation, so it does not change their relative-angle range. For radii r and u, squared separation equals $(r-u)^2 + 2ru(1-\cos\delta)$. The smallest allowed angular separation supplies the distance infimum; the largest supplies its supremum.

Propagation of specified sets is distinct from assigning distributions, as interval-analysis treatments make explicit (Moore et al., 2009). Applied interval methods similarly formulate feasible numerical sets from stated constraints (Jaulin et al., 2001). Here we solve a small problem directly. For each limiting cosine, the maximum over the radial rectangle occurs at a corner. The minimum is obtained by comparing its corners and the constrained stationary point on each edge. This avoids treating a few sampled positions as if they established global extrema.

Closed-set global optimization provides the relevant extremum perspective (Hansen and Walster, 2004). The radial quadratic is convex, permitting the finite candidate construction (Boyd and Vandenberghe, 2004). Its distance width is supremum minus infimum. A zero lower envelope means the closures touch or overlap in a way that permits a zero infimum. It does not prove that the rover stayed still; a boundary may only be approached under a particular half-open rounding convention.

The extrema are analytic solutions of the specified cell problem, evaluated with floating arithmetic. Their numerical checks below do not constitute a formal directed-rounding certificate, and neither calculation supplies calibrated bounds on unobserved physical positions.

A probabilistic localization model would answer a different question by specifying distributions and a robot-state model (Thrun et al., 2005). Nor do these envelopes provide a complete measurement-uncertainty budget of the kind addressed by the GUM (JCGM, 2008). Calibration, drift, transcription, true trajectory and correlations can all be relevant without being identified by these cells. Shared uncertain inputs require care in any subsequent error model (Carroll et al., 2006). The present results remain conditional deterministic sensitivities.

We first average pair widths within each traverse, then average the three traverses within a mission and finally give the three missions equal weight. This defines what receives equal representation (Solon et al., 2015). Each mission has three traverses, so the result also equals the mean of nine traverse means. A longer or more frequently reported history does not receive extra primary weight. Medians use the ordinary ordered-value rule, including the midpoint of two central observations, with that quantile convention stated for reuse (Hyndman and Fan, 1996).

Deleting one whole mission and reaveraging the other six traverses measures finite composition sensitivity. It does not turn three historical missions into a probability sample. Numerical assumptions, case composition and measurement uncertainty are separate sources of variation (Smith, 2013). Sampling-theory guarantees require a sampling design that these source histories do not possess (Neyman, 1934). No standard error, p-value or confidence coverage is assigned. Figure 1 connects the source support, two fixed assumptions and summaries.

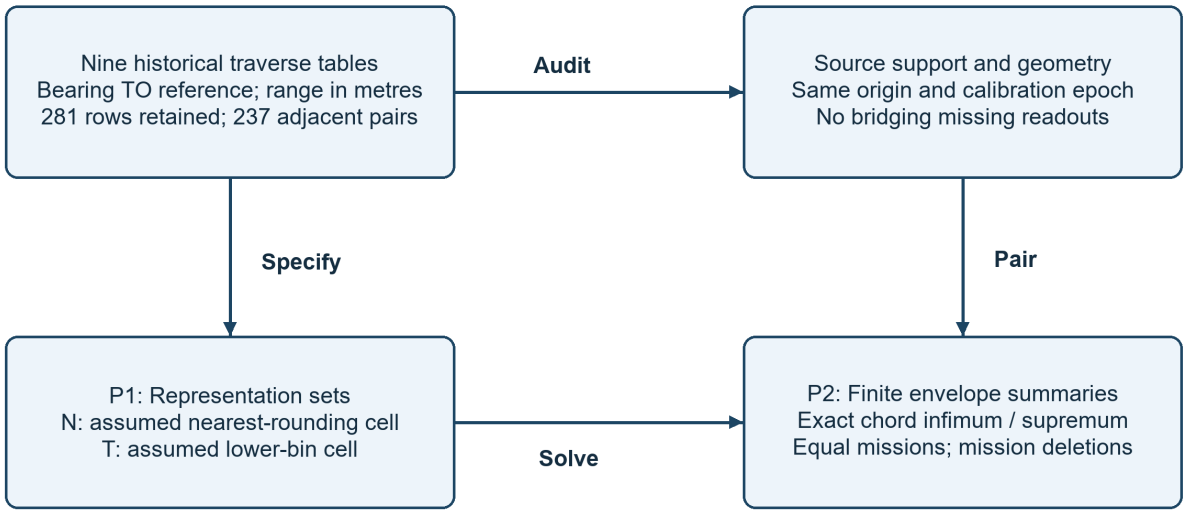


Figure 1. P1 specifies representation sets for published polar readouts; P2 summarizes the resulting distance envelopes. Both scenarios use the same 237 supported adjacent pairs from nine traverses. Arrows are analysis operations, not causal relationships or a localization algorithm.

Broad envelopes arise within every recorded traverse

The nearest-rounding width averages 175.554 m with the stated mission/traverse weights. The corresponding lower-bin width is 179.344 m, giving a T-N contrast of 3.790 m. Traverse-specific mean N widths range from 142.977 to 210.123 m. All nine traverse means appear in Table 1 and Figure 2. The result describes the two assumed cell constructions applied to the actual source geometry.

Table 1. All nine finite traverse cases and 237 supported pairs. Width is the supremum minus infimum of represented point separation. Duplicates have exactly the same printed bearing and range. The zero-infimum count is the same under N and T. These columns are deterministic geometry, not model-based uncertainty or independently replicated measurements.

Mission / traverse	Pairs	Duplicates	Median printed chord (m)	N mean width (m)	T mean width (m)	T-N mean (m)	Zero-infimum pairs
15 / 1	12	3	656.037	170.327	176.976	6.650	3
15 / 2	23	4	348.995	194.535	199.196	4.661	6
15 / 3	14	5	156.032	149.150	156.376	7.226	6
16 / 1	17	4	101.211	142.977	146.115	3.138	7
16 / 2	41	7	118.564	178.404	180.946	2.542	15
16 / 3	31	3	300.000	198.062	198.313	0.252	7
17 / 1	12	2	160.787	161.165	168.403	7.239	4
17 / 2	53	8	292.472	210.123	210.737	0.614	18
17 / 3	34	4	273.103	175.242	177.035	1.794	7

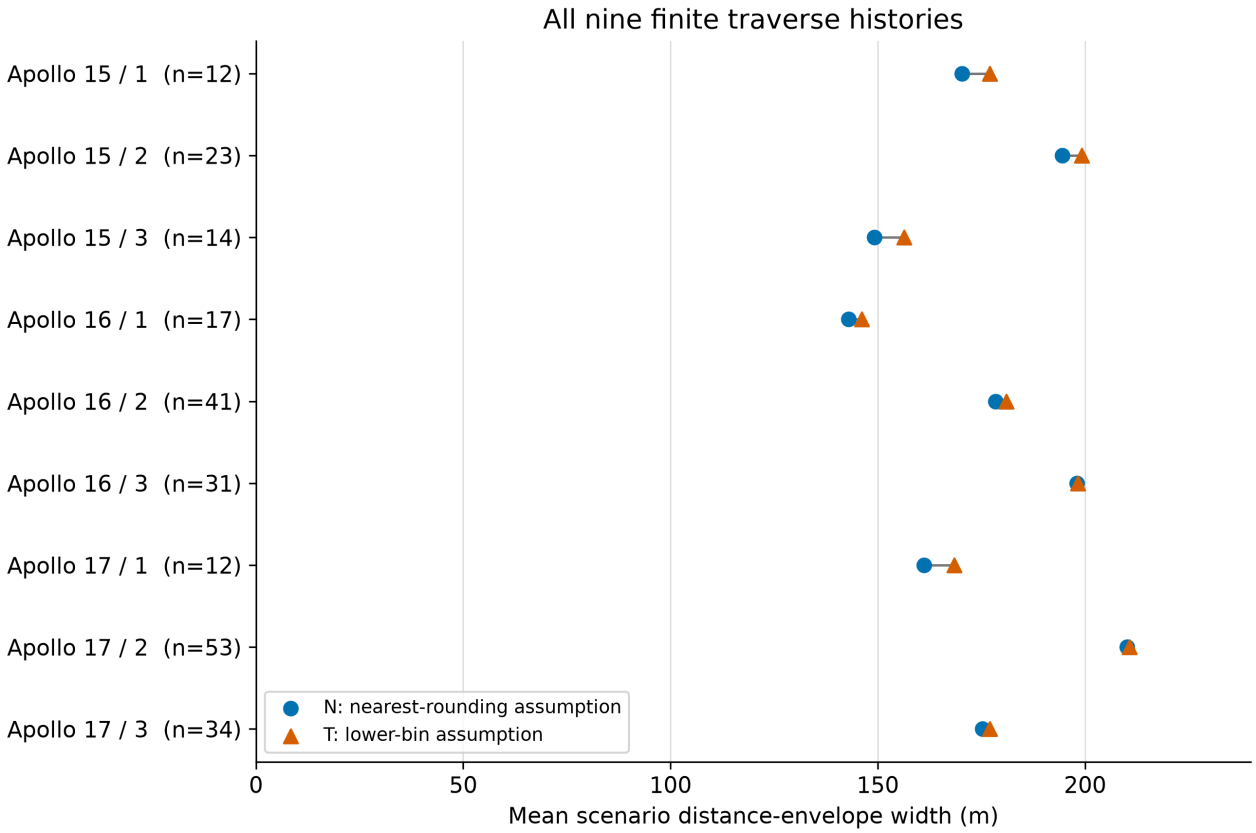


Figure 2. Mean width within every traverse on one common scale. Markers distinguish the two fixed assumptions; connectors pair the same source case. The horizontal position is an envelope width, not a true-location error bar. No inferential interval is plotted.

The scenario difference is smaller than the absolute widths, and it is not positive for every individual pair. The smallest observed T-N width contrast is -12.703 m. The two radial-cell constructions are shifted alternatives rather than nested sets; changing them can narrow some chord envelopes while widening others. A positive average therefore neither establishes a universally conservative quantizer nor identifies which historical rule was used.

Whole-mission deletion leaves N means from 172.242 to 177.662 m and T means from 176.320 to 181.454 m. The T-N mean contrast spans 2.596-4.697 m across the three omissions. Table 2 attaches these finite ranges directly to the summaries. They say how this collection's weighting changes when a named mission is removed, without predicting another mission's envelope.

Table 2. Primary finite effects and deterministic composition ranges. Scope is three missions, nine traverses and the same 237 supported pairs under each scenario. Deletion retains six traverses from two missions. No range is a confidence interval or an accuracy bound.

Quantity	Equal-mission summary (m)	Delete-one-mission range (m)
N mean width	175.554	172.242 to 177.662
T mean width	179.344	176.320 to 181.454
T-N width contrast	3.790	2.596 to 4.697

There are 40 exact printed-duplicate pairs and 197 other pairs, all with positive nominal chords in this source. The duplicate pairs have zero infima, but 33 positive printed chords also have zero infima. Overall, 73 of 237 pairs have zero infima under each assumption. The equal-mission fraction is 31.352%;

the pooled fraction is 30.802%. These differ because they answer differently weighted questions, not because one discards observations.

Table 3. Pooled record-level diagnostic, separate from the equal-mission primary estimand. Both strata retain their dependence within traverses. Other readouts means nonidentical printed coordinates; it does not certify physical movement. Fractions describe zero distance infima of scenario-cell closures.

Printed readout stratum	Pairs	N mean width (m)	T mean width (m)	Zero-infimum fraction
printed_duplicates	40	106.695	114.523	1.000
other_readouts	197	199.250	200.879	0.168

The matching zero-infimum counts do not validate either rounding rule. Both constructions have the same relative angular interval, and the source ranges occur on the documented 100 m grid. Their overlap patterns can therefore coincide even while distance widths differ. The actual counts measure how often this happens in these records. They do not estimate the probability of movement, the chance of a wrong position or a failure rate.

A repeated arrival and departure value is retained because it documents what was printed at two source events. Its inclusion does not assert an independently observed stationary period. Likewise, a change in the printed coordinates is not automatically an independently confirmed movement. The duplicate stratum describes a literal property of the archive. Missing intermediate values and irregular reporting also prevent these counts from becoming time fractions: the denominator is supported pairs, not seconds of rover operation or a uniformly sampled trajectory.

What can be reused from the reconstruction

The protocol was frozen after source inspection and before the displacement calculations. Independent checks return to separately keyed original-page values, recompute point chords with the cosine rule and solve the radial minimum through a different clipped-quadratic reduction. Seventy-digit decimal arithmetic independently evaluates the angular functions. All 474 scenario envelopes agree with the primary calculation within 1.5×10^{-11} m. That discrepancy concerns numerical implementation, not source accuracy. Numerical stability and floating-point limitations remain distinct from the uncertainty of a measurement (Higham, 2002) (Goldberg, 1991).

The complete row/status audit prevents a plausible line from concealing missing information. Field definitions and fitness for a consumer's question are part of data quality (Wang and Strong, 1996). A continuous route used in motion planning has additional geometric and physical constraints (LaValle, 2006). Sparse chords cannot recover its length, small deviations around obstacles or the distance registered by wheel odometers. Even an exact solution of the reported-cell problem cannot supply those unobserved quantities.

The acquisition record, original files, unit interpretations, origin epochs, both scenarios, code and actual output checksums remain linked. This supports computational reproducibility (Peng, 2011) and traceable reuse under FAIR principles (Wilkinson et al., 2016). It supplies a bounded result for nine historical navigation tables: a specified coordinate-display interpretation can yield substantial chord-width sensitivity while leaving actual localization and driven paths unidentified. No new model, field experiment or operating procedure is proposed. Accountable human source verification and final approval remain pending.

References

1. de Berg, Mark; Cheong, Otfried; van Kreveld, Marc; Overmars, Mark. (2008). Computational Geometry: Algorithms and Applications. Springer Berlin Heidelberg. https://doi.org/10.1007/978-3-540-77974-2
2. Borenstein, Johann; Feng, Liqiang. (1996). Measurement and correction of systematic odometry errors in mobile robots. IEEE Transactions on Robotics and Automation,12(6),869-880. https://doi.org/10.1109/70.544770
3. Carroll, Raymond J., David Ruppert, Leonard A. Stefanski, and Ciprian M. Crainiceanu. “Measurement Error in Nonlinear Models.” 2006. https://doi.org/10.1201/9781420010138.
4. Neyman, Jerzy. (1934). On the Two Different Aspects of the Representative Method: The Method of Stratified Sampling and the Method of Purposive Selection. Journal of the Royal Statistical Society,97(4),558-606. https://doi.org/10.1111/j.2397-2335.1934.tb04184.x.
5. Volder, Jack E.. (1959). The CORDIC Trigonometric Computing Technique. IRE Transactions on Electronic Computers. https://doi.org/10.1109/tec.1959.5222693
6. Boyd, Stephen; Vandenberghe, Lieven. (2004). Convex Optimization. Cambridge University Press. https://doi.org/10.1017/cbo9780511804441
7. Hyndman, Rob J.; Fan, Yanan. (1996). Sample Quantiles in Statistical Packages. The American Statistician. https://doi.org/10.1080/00031305.1996.10473566
8. Widrow, Bernard; Kollár, István. (2008). Quantization Noise: Roundoff Error in Digital Computation, Signal Processing, Control, and Communications. Cambridge University Press. https://doi.org/10.1017/cbo9780511754661
9. Xiao, Xin-Yu; Tian, Ye; He, Zhixian; Chen, Qilin; Wang, Shiqi; Xia, Qianchen. (2026). Lunar-R1: Towards Efficient Reasoning of Large Language Models for Lunar Exploration via Reinforcement Learning. Proceedings of the 2026 Conference on Empirical Methods in Natural Language Processing: Industry Track. https://aclanthology.org/2026.emnlp-industry.5/.
10. Thrun, Sebastian; Burgard, Wolfram; Fox, Dieter. (2005). Probabilistic Robotics. MIT Press. ISBN9780262201629. https://mitpress.mit.edu/9780262201629/probabilistic-robotics/
11. Wilkinson, Mark D.; Dumontier, Michel; Aalbersberg, IJsbrand Jan; Appleton, Gabrielle; Axton, Myles; Baak, Arie; Blomberg, Niklas; Boiten, Jan-Willem; da Silva Santos, Luiz Bonino; Bourne, Philip E.; Bouwman, Jildau; Brookes, Anthony J.; Clark, Tim; Crosas, Mercè; Dillo, Ingrid; Dumon, Olivier; Edmunds, Scott; Evelo, Chris T.; Finkers, Richard; Gonzalez-Beltran, Alejandra; Gray, Alasdair J.G.; Groth, Paul; Goble, Carole; Grethe, Jeffrey S.; Heringa, Jaap; ’t Hoen, Peter A.C; Hooft, Rob; Kuhn, Tobias; Kok, Ruben; Kok, Joost; Lusher, Scott J.; Martone, Maryann E.; Mons, Albert; Packer, Abel L.; Persson, Bengt; Rocca-Serra, Philippe; Roos, Marco; van Schaik, Rene; Sansone, Susanna-Assunta; Schultes, Erik; Sengstag, Thierry; Slater, Ted; Strawn, George; Swertz, Morris A.; Thompson, Mark; van der Lei, Johan; van Mulligen, Erik; Velterop, Jan; Waagmeester, Andra; Wittenburg, Peter; Wolstencroft, Katherine; Zhao, Jun; Mons, Barend. (2016). The FAIR Guiding Principles for scientific data management and stewardship. Scientific Data. https://doi.org/10.1038/sdata.2016.18.
12. Wang, Richard Y.; Strong, Diane M.. (1996). Beyond Accuracy: What Data Quality Means to Data Consumers. Journal of Management Information Systems. https://doi.org/10.1080/07421222.1996.11518099
13. Moore, Ramon E.; Kearfott, R. Baker; Cloud, Michael J.. (2009). Introduction to Interval Analysis. Society for Industrial and Applied Mathematics. https://doi.org/10.1137/1.9780898717716
14. Bennett, W. R.. (1948). Spectra of Quantized Signals. Bell System Technical Journal. https://doi.org/10.1002/j.1538-7305.1948.tb01340.x
15. Smith, Ralph C.. (2013). Uncertainty Quantification: Theory, Implementation, and Applications. Society for Industrial and Applied Mathematics. https://doi.org/10.1137/1.9781611973228
16. Goldberg, David. (1991). What every computer scientist should know about floating-point arithmetic. ACM Computing Surveys. https://doi.org/10.1145/103162.103163
17. Solon, Gary; Haider, Steven J.; Wooldridge, Jeffrey M.. (2015). What Are We Weighting For?. Journal of Human Resources. https://doi.org/10.3368/jhr.50.2.301.
18. Hansen, Eldon; Walster, G. William, editors. (2004). Global Optimization Using Interval Analysis: Revised and Expanded,2nd edition. CRC Press. ISBN9780824740597. https://doi.org/10.1201/9780203026922
19. Stevens, S. S.. (1946). On the Theory of Scales of Measurement. Science. https://doi.org/10.1126/science.103.2684.677.
20. Smith, Earnest C.; Mastin, William C. (1973). Lunar Roving Vehicle Navigation System Performance Review. NASA Technical Note D-7469. NASA Marshall Space Flight Center. https://ntrs.nasa.gov/citations/19740003321

21. LaValle, Steven M.. (2006). Planning Algorithms. Cambridge University Press. https://doi.org/10.1017/cbo9780511546877
22. Joint Committee for Guides in Metrology. (2012). International vocabulary of metrology - Basic and general concepts and associated terms (VIM), third edition (JCGM200:2012). Bureau International des Poids et Mesures. https://doi.org/10.59161/JCGM200-2012
23. Gray, R.M.; Neuhoff, D.L.. (1998). Quantization. IEEE Transactions on Information Theory. https://doi.org/10.1109/18.720541
24. Joint Committee for Guides in Metrology. (2008). Evaluation of measurement data - Guide to the expression of uncertainty in measurement (JCGM100:2008). Bureau International des Poids et Mesures. https://doi.org/10.59161/JCGM100-2008E
25. Bureau International des Poids et Mesures. (2019). The International System of Units (SI),9th edition,version3.01(August2024). https://www.bipm.org/documents/20126/41483022/SI-Brochure-9-EN.pdf/2d2b50bf-f2b4-9661-f402-5f9d66e4b507?version=4.0
26. Mardia, Kanti V.; Jupp, Peter E.. (1999). Directional Statistics. Wiley Series in Probability and Statistics. https://doi.org/10.1002/9780470316979
27. Planetary Data System Geosciences Node. (n.d.). Apollo Analyst's Notebook: Map-Basemap Generation and Traverse Generation. Washington University in St. Louis. https://an.rsl.wustl.edu/apollo/data/userguide/map.htm
28. Higham, Nicholas J.. (2002). Accuracy and Stability of Numerical Algorithms: Second Edition. Society for Industrial and Applied Mathematics. https://doi.org/10.1137/1.9780898718027
29. Peng, Roger D.. (2011). Reproducible Research in Computational Science. Science. https://doi.org/10.1126/science.1213847
30. Jaulin, Luc; Kieffer, Michel; Didrit, Olivier; Walter, Éric. (2001). Applied Interval Analysis. Springer London. https://doi.org/10.1007/978-1-4471-0249-6